Supplementary Data

Surface Modification Engineering of Two-dimensional Titanium Carbide for Efficient Synergistic Multitherapies of Breast Cancer

Lei Bai [a], Wenhui Yi *[a], Taiyang Sun [b], Yilong Tian [a], Ping Zhang [c], Jinhai Si [a], Xun Hou [a], Jin Hou *[b]

[a] School of Electronic Science and Engineering, Faculty of Electronic and Information Engineering, Xi'an Jiaotong University, Xi'an, Shaanxi 710049, China

[b] Department of Pharmacology, School of Basic Medical Sciences, Xi'an Medical University, Xi'an 710021, Shaanxi, People's Republic of China

[c] College of science, Northwest A&F University, Xi'an 712100, Shaanxi, People's Republic of China

E-mail addresses: yiwenhui@mail.xjtu.edu.cn (W. Yi), 1127538475@qq.com (J. Hou)

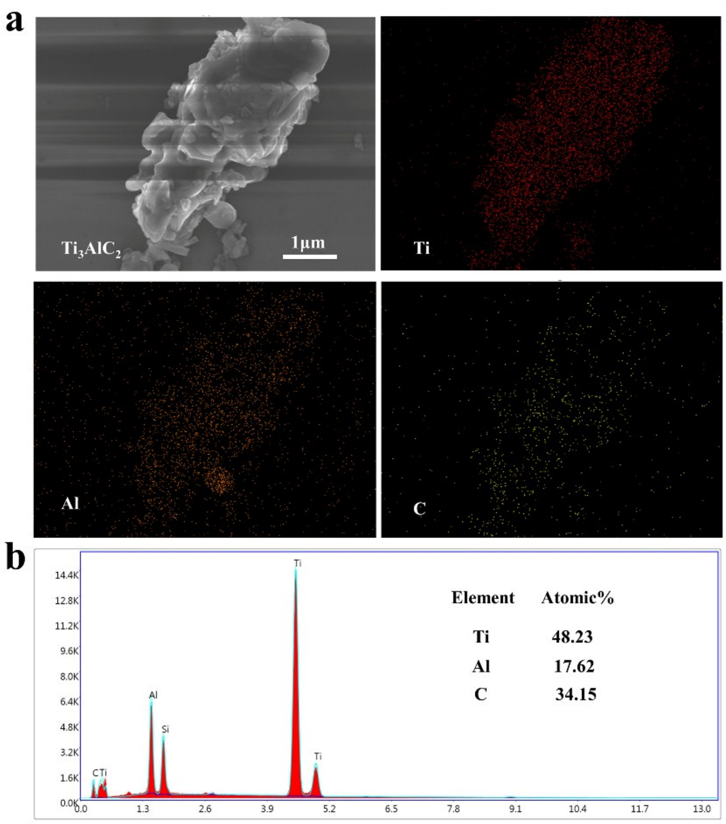

Fig. S1. (a) SEM images of Ti_3AlC_2 and element mapping images. (b) corresponding X-ray energy dispersive spectroscopy (EDS).

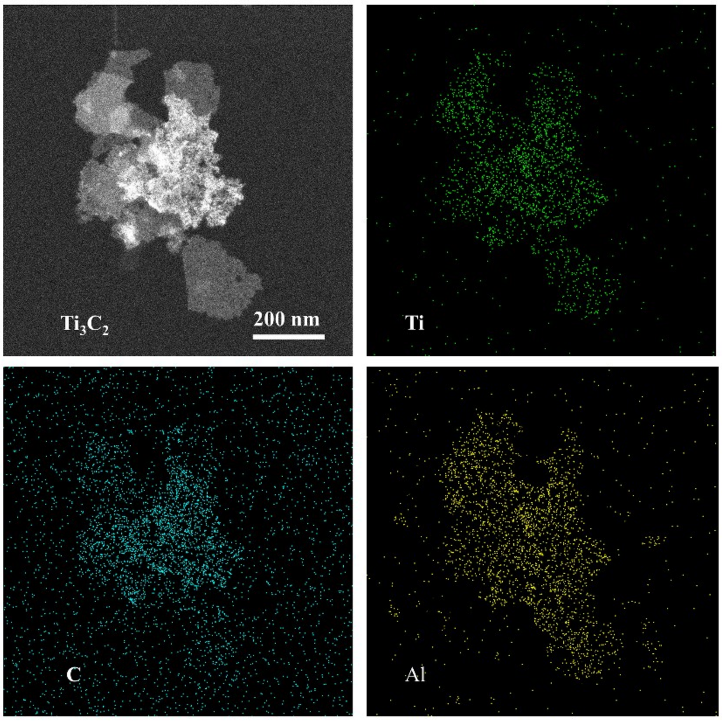

Fig. S2. SEM elemental mapping of $Al(OH)_4^-$ functionalized Ti_3C_2 nanosheets synthesized by two-step liquid exfoliation.

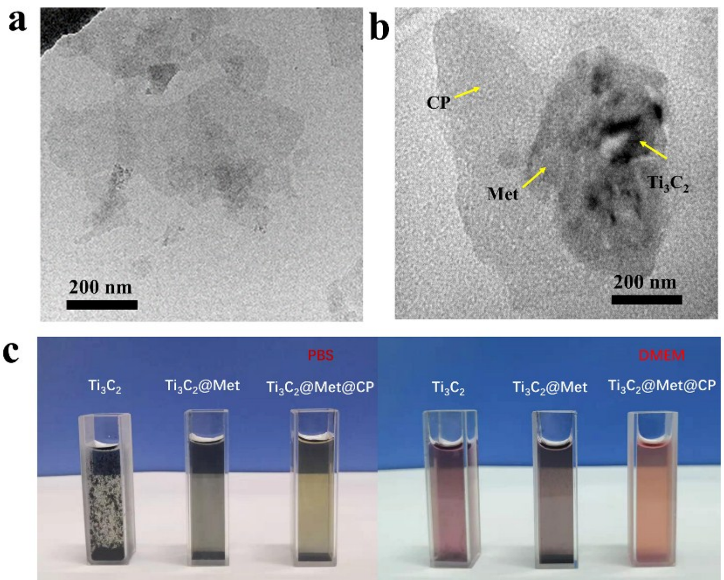

Fig. S3. (a) TEM images of Ti_3C_2 nanosheets after exfoliation. (b) High-resolution SEM image of Ti_3C_2@Met@CP. (c) Photographs of Ti_3C_2, Ti_3C_2@Met and Ti_3C_2@Met@CP dispersed in various solutions (PBS, DMEM).

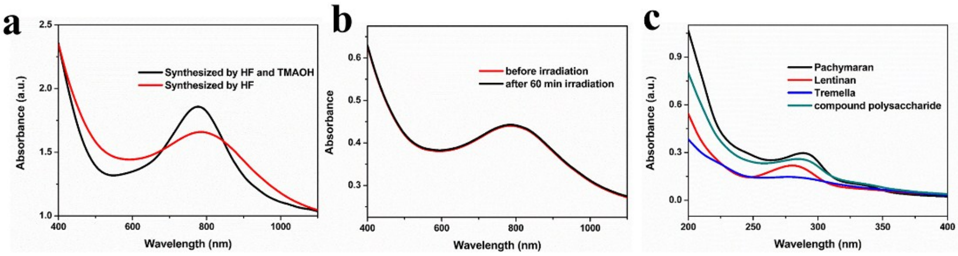

Fig. S4. (a) UV−vis absorbance of Ti_3C_2 nanosheets with/without TMAOH intercalation step during exfoliation. (b) UV-vis absorption spectra of Ti_3C_2 nanosheets before and after 60 min irradiation of 808 nm laser. (c) The absorption spectra confirmed that Lentinan, Pachymaran and Tremella polysaccharide were combined to form compound polysaccharide (CP).

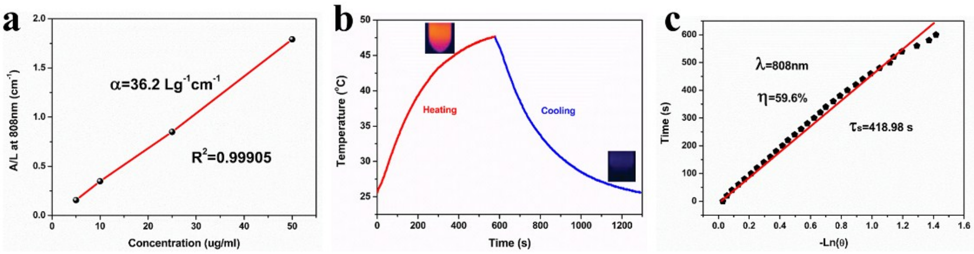

Fig. S5. (a) Mass extinction coefficient of Ti_3C_2 nanosheets at 808 nm. Normalized absorbance intensity at λ = 808 nm divided by the characteristic length of the cell (A/L) at varied concentrations (5, 10, 25, 50μg mL^{-1}). (b) Photothermal effect of an aqueous dispersion of Ti_3C_2@Met@CP under 808 nm laser irradiation. (c) Time constant for heat transfer from the system was determined to be τ_s= 418.98 s by using the linear time data from the cooling period versus negative natural logarithm of driving force temperature, which was obtained from the cooling stage.

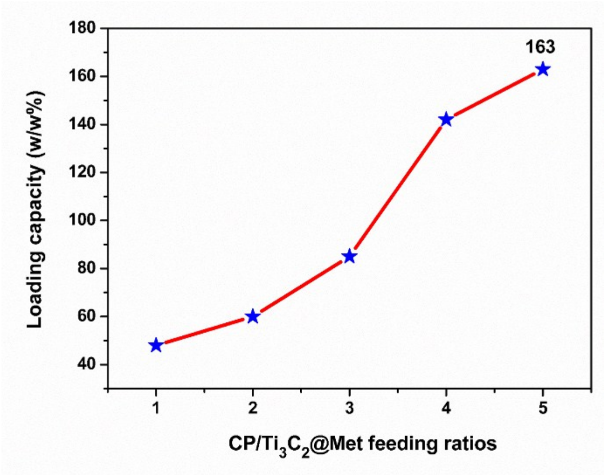

Fig. S6. CP-Coating capacities of Ti_3C_2@Met composite nanosheets at different CP/Ti_3C_2@Met ratios.

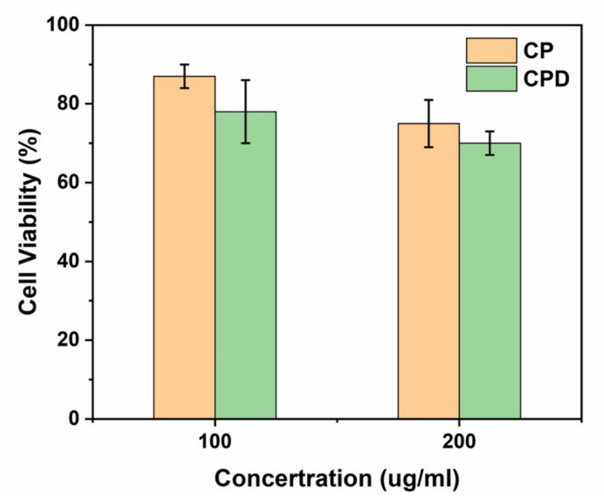

Fig. S7. Cell Viability after co-incubation CP and CPD (100, 200μg mL^{-1}) with MDA-MB-231 cells.

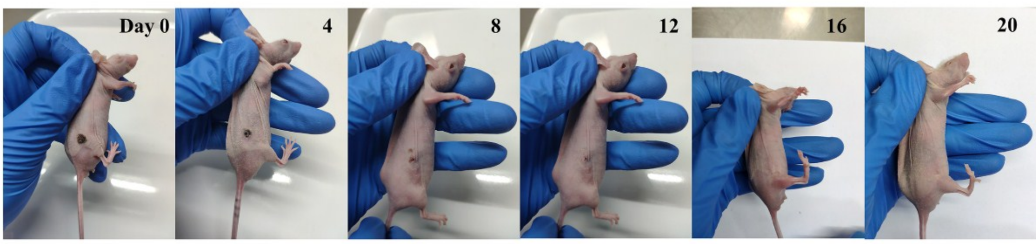

Fig. S8. Photographs of tumor-bearing mice within 20 days after Ti_3C_2@Met@CP +Laser treatment.

Groups	Proportion			Inhibition rate (%)
	Lentinan	Pachymaran	Tremella polysaccharide	
Blank control group	0	0	0	0
1	0	0	1	7.8
2	2	0	1	10.7
3	0	2	1	8.6
4	2	2	1	16.2
5	0	1	0	5.5
6	2	1	0	11.8
7	0	1	2	7.8
8	2	1	2	25.1
9	1	0	0	4.7
10	1	2	0	10.1
11	1	0	2	13.3
12	1	2	2	16.7
13	1	1	1	8.4
14	1	1	1	8
15	1	1	1	8.3

Table S1. The growth inhibitory effect of compound polysaccharide with different proportion on MDA-MB-231 cells. (The final concentration of the compound polysaccharide was determined to be 200μg mL^{-1}).

	IC_{50} (μg mL^{-1})		
	Ti_3C_2	Ti_3C_2@Met	Ti_3C_2@Met@CP
No laser	429.5±8.3	213.3±6.1	187.5±5.2
1W cm^{-2} (808nm)	55.7±4.3	41.9±3.7	33.4±3.9

Table S2. The IC_{50} values of Ti_3C_2, Ti_3C_2@Met, and Ti_3C_2@Met@CP on MDA-MB-231 cells after with laser (1W cm^{-2}, 808nm) and without laser treatment.